Maturing broadband 3D CSEM for improved reservoir property prediction in the Realgrunnen Group at Wisting, Barents Sea

John Reidar Granli and Helene Hafslund Veire, OMV Norge, Pål T. Gabrielsen and Jan Petter Morten, EMGS*

Summary

In this paper we describe the highlights from a wide range of CSEM applications and developments in the Wisting area. At an initial stage, by including higher frequencies in 3D CSEM inversion at Wisting, we realized that our CSEM data contained a lot more detailed information about reservoir properties than earlier anticipated. Beyond the traditional application of predicting high vs. low hydrocarbon saturation, the CSEM data are used for estimation of hydrocarbon column and is starting to be used in estimation of reservoir heterogeneity and even connectivity. Our quantitative workflows are still maturing and are expected to provide future value. At Wisting we have been fortunate to be in an active appraisal setting where new wells have repeatedly provided calibration and adjustment to our CSEM workflows. During almost four years we have acquired two field-scale tailored 3D CSEM surveys with gradually denser spatial sampling and higher frequencies. These have provided higher accuracy and better spatial resolution than the conventional coarse-grid survey design used in multi-client projects. Our project work has been highly cross-disciplinary, where CSEM expertise paired with specialists in rock physics, seismic AVO and geology has worked very well. Our ability to operate as one team across company barriers is a key success factor with learning, re-learning and geoscience integration as main ingredients.

Introduction

The Wisting field is located in the Hoop fault complex and was discovered by the Central well in 2013. The reservoir is from The Realgrunnen Subgroup (Sgr) of the Kapp Toscana Group. In the Hoop Fault Complex Area, the Realgrunnen Sgr consists of three formations: Fruholmen-, Nordmela- and Stø Fm. The Stø Fm is Late Pliensbachian to Bajocian in age, the youngest and by far the most important reservoir. It has the appearance of sandy sequences, mineralogically mature and well-sorted sandstone lithology, and exhibits excellent reservoir properties. The tectonic history has been very active with several episodes of uplift and erosion, the most marked ones during Cenozoic and Neogene times. The structural crest is currently at 250 m burial depth below a 400 m sea column, while the burial-history maximum is estimated to roughly 2000 mBML, i.e. ~1350 m of net uplift and erosion. The electric properties for oil-filled Stø are remarkable and reaches resistivity values of >100 kΩm from well measurements. The background resistivity in the area is also high, ~20 Ωm, which implies that low-resistivity low-saturated oil reservoirs may be overlooked by CSEM. With the high resistivity values seen at Wisting, detection is not a problem, as summarized for different inversion and survey vintages in Figure 1. The seismic data provide vital calibration for CSEM at Wisting, both in terms of structural and rock property constraints. Two key challenges with the current wide tow 3D seismic are worth mentioning: Being shallow and even above the first seabed multiple is good, but also very challenging for AVO analysis due to low fold and very poor angle sampling across small angle bins. We have also found that the Poisson ratio estimated from wireline is difficult to match with the seismic data, possibly due to frequency dispersion, caused by micro-fracturing (see Veire et al., 2016).

Broadband and high resolution 3D CSEM

At the project outset, guided by high resistivity values in the discovery well, we started to think that higher frequencies than those of the commonly used waveforms would be useful to delineate the saturated reservoir or resistor. The amplitude spectra from the real data suggested that it was be feasible to invert using frequencies up to 12 Hz. The results from this "broadbanding" are summarized in Figure 1 and demonstrate improvement in structural definition and conformance for the anomalous resistors, and increased sensitivity from higher frequencies.

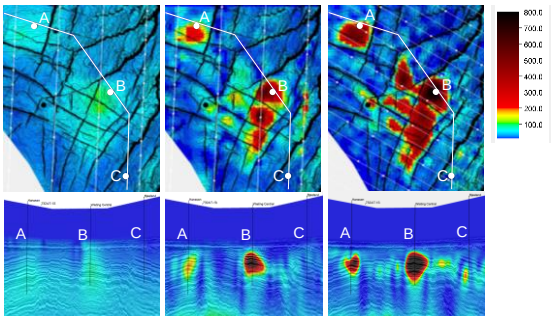

Figure 1. 3D CSEM inversion results using different frequency ranges. The images show maps (top) and sections (bottom) associated with the Realgrunnen target. Vintage data (2008) with "standard" frequency range <1.5 Hz (left), data from the same acquisition including up to 12 Hz (middle) and from a focused survey (2014) with up to 22 Hz (right). A, B and C are well locations with Realgrunnen oil, oil and wet, respectively.

Encouraged by the findings, a more focused 3D CSEM acquisition was decided. The source towline sampling decreased from 3 km to 1 km and receiver sampling went

from 3 km x 3 km to 2 km x 2 km. Combined with a higher usable frequency content (up to 22 Hz), the inversion results improved even further, as seen in Figure 1 right.

Recovering earth properties from CSEM data

Modern CSEM source and receiver hardware can deliver very accurate data and enable very specific measurement uncertainty analysis in the amplitude and phase of processed data. This makes CSEM ideal for full waveform inversion to obtain subsurface images and recover earth parameters. In our current context of high frequencies in a high-resistive background, the thin resistor guided wave condition results in a very strong measured response compared to data uncertainty. For the thin and approximately horizontal resistive layer, the CSEM source field interaction with the hydrocarbon reservoir leads to large vertical electric field strength inside the resistor that propagates with a much larger phase velocity and less attenuation than signals propagating in the background. The guided wave will couple to the surroundings, and a leakage of the field is detected at the seafloor receivers. This signature of the guided wave contains information about the propagation that is used to image the resistor, see Mittet and Morten (2013) and Constable and Weiss (2006). The response is governed by a composite earth property parameter called Anomalous Transverse Resistance (ATR) given by

$$\mathrm{ATR} = \left(R_V^{\mathrm{Resistor}} - R_V^{\mathrm{Background}}\right)\Delta z,$$

where $R_V^{\mathrm{Resistor}} - R_V^{\mathrm{Background}}$ is the vertical resistivity difference between resistor and background, and Δz is the resistor thickness. ATR is thus related to resistivity and resistor geometry in the subsurface and our starting point for building interpretation workflows to retrieve earth properties from CSEM data.

Maturing a framework for CSEM interpretation

Interpretation of CSEM data is usually performed in two stages. First the data are inverted to determine ATR, and then the ATR is interpreted (decomposed) into reservoir parameters. Various schemes exist e.g. petrophysical joint inversion (PJI) of seismic and CSEM (Miotti et al., 2013), joint interpretation of CSEM and multivariate seismic attributes analysis (Alvarez et al., 2017), and the prospectivity evaluation approach (Baltar and Barker, 2015) where ATR and background are interpreted from inverted data and a Monte Carlo simulation defines probability distributions for hydrocarbon volume controlling parameters to provide volume range quantiles. The approach taken here is different and more labor and computationally intensive. It is also iterative and scenario driven, and consists of three parts: 1) retrieve accurate geometrical constraints from seismic interpretation, 2) populate model with alternative resistivity scenarios extracted from well data, seismic and geology and 3) perform survey consistent 3D modeling and inversion of the alternative resistivity models (earth scenarios). Then compare and match to real data, and re-iterate. This implies joint interpretation with cross-disciplinary judgment. Our workflow maturation has been stepwise and in phase with Wisting appraisal wells. Early versions were tested prior to drilling the Hanssen and Bjaaland segments. 3D modeling and inversion using different resistivity scenarios was run, and Figure 2 shows the summary assessment. A large and structurally conform seismic DHI was a good reason to select Bjaaland as drilling target. The clear discrepancy in 3D CSEM between "oil-filled" synthetic scenario vs. real data suggested residual saturation to explain the seismic DHI. In spite of this, Bjaaland was still drilled, mainly due to size and modest belief in the CSEM technology at the time. The well came back with residual gas in Stø.

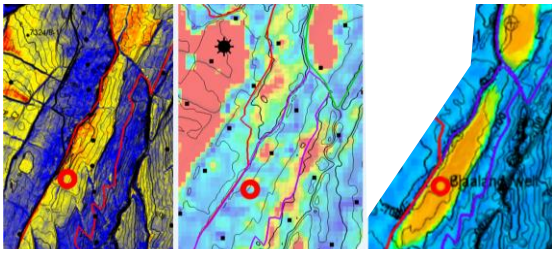

Figure 2. Geophysical responses at the Bjaaland segment. Seismic amplitude (left), average resistivity from 3D CSEM (middle) and modeled data assuming oil-saturated (right). The discrepancy between the modeled oil scenario and the real data is very high for CSEM data.

The following Central II well had two main objectives, to prove feasibility of horizontal production/injection drilling for the shallow target, and to perform production testing. The well was placed in an area with both CSEM and seismic anomaly, see Figure 3.

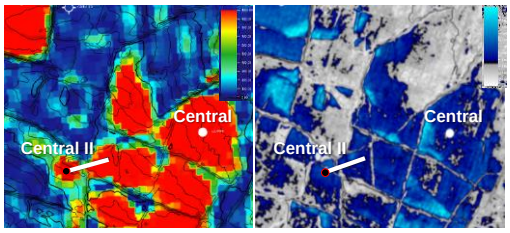

Figure 3. Projection of the deviated Central II well path (white line) onto Realgrunnen average resistivity from CSEM data (left) and seismic amplitude (right). The Central (discovery) well position is included for reference.

Prior to drilling Central II, the CSEM data were used to predict the oil water contact (OWC) in all segments across the field. The same 3-step interpretation framework was applied, still assuming homogeneous resistivity in oil

saturated reservoir with varying OWC. The investigation is summarized in Figure 4 with three modeled OWC levels, base case (B), base case -5 m (C) and base case +5 m (D). The real CSEM data are shown in (A) and give best match to the model base case +5 m along the planned wellbore. The high CSEM sensitivity of 5 m OWC increments was surprising and suggests an even deeper OWC in the northwest segment (white arrow). The Central II well results came back with good agreement to predictions. The downhole deep directional resistivity results suggesting OWC at base case +5 m is shown in Figure 4 (bottom), i.e. a very good match to CSEM. A more detailed calibration of CSEM vs. well deep directional resistivity measurements is given in Morten et al. (2017). Our next workflow steps are taking us towards predicting saturation quantitatively. We are currently investigating "how quantitative" it is possible to be based on the ATR approximation given by

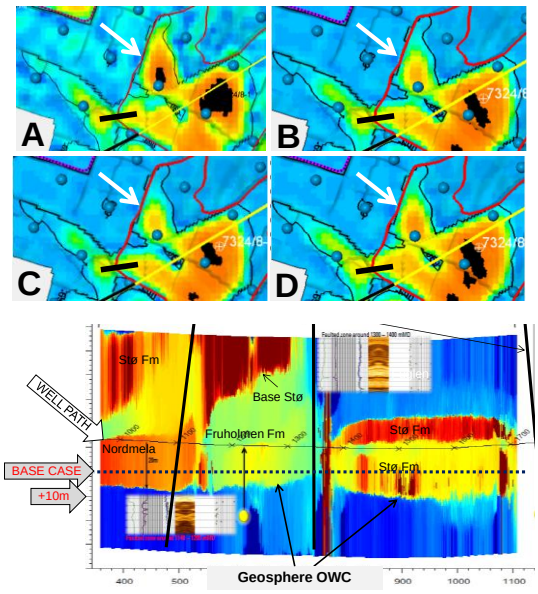

Figure 4. Realgrunnen average resistivity for real 3D CSEM data (A), 3D modeling and inversion of base case (B), based case -5m (C) and base case +5m (D). The geosteering results from Central II showing resistivity profiles along the deviated well path (black line) suggests a deeper OWC than base case.

$$\mathrm{ATR} = \int_{\mathrm{OWC}}^{\text{Top reservoir}} R_V\big(S_W(z)\big)dz - R_V^{\text{Background}}\Delta z,$$

where $S_W(z)$ is the water saturation varying with height of the hydrocarbon column and highly dependent on reservoir quality. The vertical resistivity $R_V(S_W)$ depends on water saturation and hence hydrocarbon column height. The ATR correspondence to reservoir quality and column height dependence including saturation ramp-up is summarized for different Wisting reservoirs in Figure 5. As an example, ATR=10 kΩm may imply a range of column heights between 10-30 m, depending on reservoir properties.

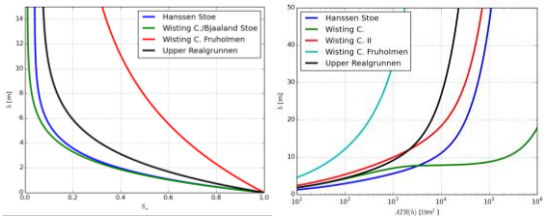

Figure 5.Saturation transition curves (left) and ATR curves (right) as a function of column height above OWC for different reservoirs representative of wells at Wisting.

Reservoir quality thus needs to be accounted for in order to make a proper ATR decomposition to extract resistivity and eventually saturation. A key step is to include internal Realgrunnen stratigraphy in the 3D resistivity model. In Figure 6 each sub-layer is populated with resistivity values estimated from well data and assigned to layers mapped from seismic. Note that there is still not a proper account for saturation ramp-up, but this is in progress. In Figure 6 a few of the 3D modeling and inversion scenarios are shown in comparison to real data. A consistently good match is achieved to the left of the horst, while the current range of models is still not matching well within and beyond the horst. These early results demonstrate a high sensitivity of 3D CSEM data to small scale variation in reservoir properties and is clearly encouraging going forward with even more detailed models, including proper handling of saturation ramp-up and even accounting for fault properties that may be significant.

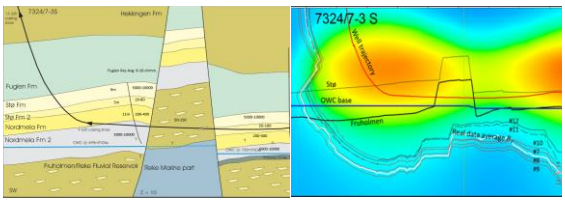

Figure 6. A stratified geosection along the Central II well traverse with resistivity model based on seismic and well data (left). Average resistivity from 3D CSEM modeling based on alternative Realgrunnen reservoir scenarios (black curves) overlaid by the real 3D CSEM response (white curve), with increasing resistivity downwards.

Survey optimization and the limits for target imaging

Close to Wisting there is additional exploration acreage in the same Realgrunnen play. The geophysical setting is illustrated in Figure 7, showing even brighter seismic

anomalies, but weaker CSEM anomalies than at Wisting. With lower structural relief and smaller column, and also alternative reservoir models (ref Figure 5), this could still work. Motivated by our recent learning on increased sensitivity, accuracy and resolution for 3D CSEM data gained by denser spatial sampling and higher frequencies, a 3D survey design modeling was kicked off with the results summarized in Figure 8. Note the higher degree of model recovery by using more extensive spatial sampling at higher frequency compared to the 2010 vintage survey

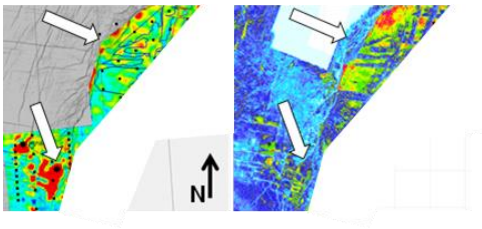

Figure 7. Comparison of 3D CSEM (left) and seismic (right) response at Realgrunnen reservoir level at Wisting and nearby exploration acreage to the northeast.

design. These results led to a full scale acquisition in the field, using a receiver spacing at 1 km and towlines at 500 m spacing. The source waveform used frequencies in the range 4-48Hz. In comparison the 2010 vintage survey used 3 km source and receiver spacing at frequency range 1-22 Hz. In total 281 receivers were deployed with 51 towlines and 1015 km towing. Early results from this survey are shown in Figure 9, confirming the predicted effect of increased resolution and sensitivity for CSEM anomalies with low ATR anomalies. We expect to retrieve more accurate reservoir parameter estimates from this.

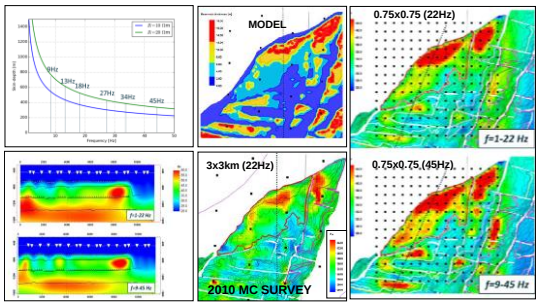

Figure 8. 3D CSEM model recovery using modeling and inversion based on alternative survey designs in a low ATR exploration acreage north east of Wisting.

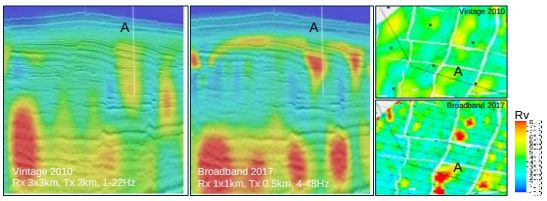

Figure 9. 3D CSEM unconstrained inversion (preliminary) using vintage vs. new broadband data. Cross section views (left) and map views with Realgrunnen projection (right).

Learning and conclusion

Our story started with the Wisting discovery in 2013, and we could rationalize and say that Wisting is so special and that by gravity of a large oil discovery "things" will start happening by themselves. In the introduction to her book Teaming, Amy Edmondsson (2012) states the following: "Most people recognize that the knowledge-based twenty first century organizations depend on cross-disciplinary collaboration, flattened hierarchies and continuous innovation. One reason for this is that the expertise has splintered into subfields. Unfortunately, the problems that need solving haven't narrowed accordingly." Recognizing the need for sharing and integration is a good start. Living and enduring it over time, as we have done in our multi-year endeavor project on CSEM integration, is rewarding and functions much in line with a favored organizational design for effective integration devised by Edmondsson with teaming, organizing to learn, execution as learning as key ingredients. We have demonstrated that investment in detailed joint analysis and integration of CSEM and seismic data can provide a lot more information about reservoir properties than earlier anticipated. We are still in the middle of "execution as learning" with a clear goal to demonstrate that accurate quantitative prediction is possible by CSEM data. Another learning is also that CSEM technology adoption is stimulated when internal stakeholders gain good understanding of details in the value chain, from wave phenomena via data processing, inversion, ATR decomposition and reservoir property prediction. This takes much effort, but less than that, may hamper proper adoption.

Acknowledgement

We thank OMV Norge and EMGS for permission to publish this information. We also thank the partners in PL537 (Statoil, Idemitsu and Petoro) for support. Eirik Stueland, Peter Berger, Kristoffer Birkeland, Michael Behm, Lars Lorenz, Bård Sigvathsen and Romain Corseri are acknowledged for their contribution in various phases of the project.

EDITED REFERENCES

Note: This reference list is a copyedited version of the reference list submitted by the author. Reference lists for the 2017 SEG Technical Program Expanded Abstracts have been copyedited so that references provided with the online metadata for each paper will achieve a high degree of linking to cited sources that appear on the Web.

REFERENCES

Alvarez, P., A. Alvarez, L. Macgregor, F. Bolivar, R. Keirstead, and T. Martin, 2017, Reservoir properties integrating controlled-source electromagnetic, prestack seismic and well log data using a rock-physics framework: Case study in the hoop Area, Barents Sea, Norway: Interpretation, **5**, SE43–SE60, https://doi.org/10.1190/INT-2016-0097.1.

Baltar, D., and N. D. Barker, 2015, Prospectivity evaluation with CSEM: First Break, **33**, 33–41.

Edmondson, A. C., 2012, Teaming: Jossey-Bass.

Miotti, F., I. Guerra, F. Ceci, A. Lovatini, M. Paydayesh, M. Leathard, and A. Sharma, 2013, Petrophysical Joint Inversion of seismic and EM attributes: A case study: 83th Annual International Meeting, SEG, Expanded Abstracts, 2516–2521, http://doi.org/10.1190/segam2013-0877.1.

Mittet, R., and J. P. Morten, 2013, The marine controlled-source electromagnetic method in shallow water: Geophysics, **78**, no. 2, E67–E77, http://doi.org/10.1190/geo2012-0112.1.

Morten, J. P., H. Veire, J. R. Granli, and P. T. Gabrielsen, 2017, Quantitative comparison of deep-reading well resistivity to 3D CSEM at Wisting: 87th Annual International Meeting, SEG, Expanded Abstracts.

Veire, H., J. R. Granli, P. Berger, O. Lewis, M. Hohner, T. Kvist-Lassen, P. Smith, and L. Stuberg, 2016, The wisting discovery–Integrating acoustic measurements at different scales: 78th Annual International Conference and Exhibition, EAGE, Extended Abstracts, http://doi.org/10.3997/2214-4609.201601552.

Weiss, C. J., and S. Constable, 2006, Mapping thin resistors and hydrocarbons with marine EM methods, Part II—Modeling and analysis in 3D: Geophysics, **71**, no. 6, G321–G332, http://doi.org/10.1190/1.2356908.